

## Search for the Weak Decay of a Lightly Bound $H^0$ Dibaryon

A. Alavi-Harati,<sup>12</sup> T. Alexopoulos,<sup>12</sup> M. Arenton,<sup>11</sup> K. Arisaka,<sup>2</sup> S. Averitte,<sup>10</sup> A. R. Barker,<sup>5</sup> L. Bellantoni,<sup>7</sup> A. Bellavance,<sup>9</sup> J. Belz,<sup>10</sup> R. Ben-David,<sup>7,\*†</sup> D. R. Bergman,<sup>10</sup> E. Blucher,<sup>4</sup> G. J. Bock,<sup>7</sup> C. Bown,<sup>4</sup> S. Bright,<sup>4</sup> E. Cheu,<sup>1</sup> S. Childress,<sup>7</sup> R. Coleman,<sup>7</sup> M. D. Corcoran,<sup>9</sup> G. Corti,<sup>11</sup> B. Cox,<sup>11</sup> M. B. Crisler,<sup>7</sup> A. R. Erwin,<sup>12</sup> R. Ford,<sup>7</sup> A. Glazov,<sup>4</sup> A. Golossanov,<sup>11</sup> G. Graham,<sup>4</sup> J. Graham,<sup>4</sup> K. Hagan,<sup>11</sup> E. Halkiadakis,<sup>10</sup> K. Hanagaki,<sup>8</sup> S. Hidaka,<sup>8</sup> Y. B. Hsiung,<sup>7</sup> V. Jejer,<sup>11</sup> D. A. Jensen,<sup>7</sup> R. Kessler,<sup>4</sup> H. G. E. Kobrak,<sup>3</sup> J. LaDue,<sup>5</sup> A. Lath,<sup>10</sup> A. Ledovskoy,<sup>11</sup> P. L. McBride,<sup>7</sup> A. P. McManus,<sup>11</sup> P. Mikelsons,<sup>5</sup> E. Monnier,<sup>4,\*‡</sup> T. Nakaya,<sup>7</sup> K. S. Nelson,<sup>11</sup> H. Nguyen,<sup>7</sup> V. O'Dell,<sup>7</sup> M. Pang,<sup>7</sup> R. Pordes,<sup>7</sup> V. Prasad,<sup>4</sup> C. Qiao,<sup>4</sup> B. Quinn,<sup>4</sup> E. J. Ramberg,<sup>7</sup> R. E. Ray,<sup>7</sup> A. Roodman,<sup>4</sup> M. Sadamoto,<sup>8</sup> S. Schnetzer,<sup>10</sup> K. Senyo,<sup>8</sup> P. Shanahan,<sup>7</sup> P. S. Shawhan,<sup>4</sup> W. Slater,<sup>2</sup> N. Solomey,<sup>4</sup> S. V. Somalwar,<sup>10</sup> R. L. Stone,<sup>10</sup> I. Suzuki,<sup>8</sup> E. C. Swallow,<sup>4,6</sup> S. A. Taegar,<sup>1</sup> R. J. Tesarek,<sup>10</sup> G. B. Thomson,<sup>10</sup> P. A. Toale,<sup>5</sup> A. Tripathi,<sup>2</sup> R. Tschirhart,<sup>7</sup> Y. W. Wah,<sup>4</sup> J. Wang,<sup>1</sup> H. B. White,<sup>7</sup> J. Whitmore,<sup>7</sup> B. Winstein,<sup>4</sup> R. Winston,<sup>4</sup> T. Yamanaka,<sup>8</sup> and E. D. Zimmerman<sup>4</sup>

(KTeV Collaboration)

<sup>1</sup>University of Arizona, Tucson, Arizona 85721

<sup>2</sup>University of California at Los Angeles, Los Angeles, California 90095

<sup>3</sup>University of California at San Diego, La Jolla, California 92093

<sup>4</sup>The Enrico Fermi Institute, The University of Chicago, Chicago, Illinois 60637

<sup>5</sup>University of Colorado, Boulder, Colorado 80309

<sup>6</sup>Elmhurst College, Elmhurst, Illinois 60126

<sup>7</sup>Fermi National Accelerator Laboratory, Batavia, Illinois 60510

<sup>8</sup>Osaka University, Toyonaka, Osaka 560, Japan

<sup>9</sup>Rice University, Houston, Texas 77005

<sup>10</sup>Rutgers University, Piscataway, New Jersey 08855

<sup>11</sup>The Department of Physics and Institute of Nuclear and Particle Physics, University of Virginia, Charlottesville, Virginia 22901

<sup>12</sup>University of Wisconsin, Madison, Wisconsin 53706

(Received 14 October 1999)

We present results of a search for a new form of hadronic matter, a six-quark, dibaryon state called the  $H^0$ , a state predicted to exist in several theoretical models. Analyzing data collected by experiment E799-II at Fermilab, we searched for the decay  $H^0 \rightarrow \Lambda p \pi^-$  and found no candidate events. We place an upper limit on  $[B(H^0 \rightarrow \Lambda p \pi^-) d\sigma_H/d\Omega]/(d\sigma_{\Xi}/d\Omega)$  and, in the context of published models, exclude the region of lightly bound mass states just below the  $\Lambda\Lambda$  mass threshold,  $2.194 < M_H < 2.231 \text{ GeV}/c^2$ , with lifetimes from  $\sim 5 \times 10^{-10} \text{ sec}$  to  $\sim 1 \times 10^{-3} \text{ sec}$ .

PACS numbers: 14.20.Pt, 12.39.Ba, 13.75.Ev, 13.85.Rm

In 1977, Jaffe [1] proposed the existence of a metastable dibaryon, the  $H^0$  (hexa-quark), a bound six-quark state ( $B = 2$ ,  $S = -2$ ), described as  $H^0 = |uuddss\rangle$ . If it exists, this hadron would be a new form of matter. The observation of a bound dibaryon would enhance the understanding of strong interactions and would aid in the search for additional exotic-multiquark states [2].

The two-flavor six-quark state is unbound [3]. Jaffe estimated that the color-hyperfine interaction between the six quarks of the three-flavor  $|uuddss\rangle$  state would be strong enough to cause the  $H^0$  to be a bound state. Different theoretical models have produced a multitude of predictions for  $M_H$ , covering a broad mass range from deeply bound states to unbound states [4]. Most of the predictions, however, are clustered in the range of  $2.1 \text{ GeV}/c^2$  up to a few  $\text{MeV}/c^2$  above the  $M_{\Lambda\Lambda}$  threshold of  $2.231 \text{ GeV}/c^2$ . If  $M_H$  is between the  $M_{\Lambda n}$  ( $2.055 \text{ GeV}/c^2$ ) and  $M_{\Lambda\Lambda}$  thresholds, it is expected to be a metastable state and undergo a  $\Delta S = 1$  weak decay. Its lifetime is estimated to be less than  $\sim 2 \times 10^{-7} \text{ sec}$  [5], while baryonic  $\Delta S =$

1 weak decays suggest a lower limit on the lifetime of  $\sim 1 \times 10^{-10} \text{ sec}$ .

Using a variety of techniques, experimentalists have been trying for years to detect the  $H^0$ , without conclusive results [6]. In recent years, production models based on empirical data with few assumptions built into them have allowed experimentalists to gauge the sensitivity of their results. In particular, the combined results from three recent experiments [6–8] rule out the mass range for  $\Delta S = 1$  transitions below  $2.21 \text{ GeV}/c^2$ . The analysis presented here covers the mass range of lightly bound  $H^0$ 's between the  $M_{\Lambda p \pi^-}$  and  $M_{\Lambda\Lambda}$  thresholds,  $2.194$  and  $2.231 \text{ GeV}/c^2$ , respectively. In addition, this search is sensitive to a large range of lifetimes, from  $\sim 5 \times 10^{-10}$  to  $\sim 1 \times 10^{-3} \text{ sec}$ , completely covering the range of lifetimes proposed in Ref. [5] yet to be probed.

It is expected that an  $H^0$  can be produced in  $pN$  collisions through hyperon production, where two strange quarks are produced, followed by the coalescence of a hyperon and a baryon to form a bound six-quark state.

Currently, the only model for  $H^0$  production at Tevatron beam energies is one proposed by Rotondo [9]. His model is based on production of the doubly strange  $\Xi^0$ , followed by the coalescence of the  $\Xi^0$  with a  $n$ , predicting a total cross section of  $1.2 \mu\text{b}$ . Our search for the  $H^0$  is the first search to normalize to the doubly strange  $\Xi^0$ , removing the strangeness production portion from the  $H^0$  production process, making this analysis a sensitive probe of hyper-nuclear coalescence.

The KTeV beam line and detector at Fermilab were designed for high precision studies of direct  $CP$  violation in the neutral kaon system (E832) and in rare  $K_L$  decays (E799-II). To reduce backgrounds from long lived neutral states, the apparatus was situated far from the production target. A clean neutral beam, powerful particle identification, and very good resolution for both charged particles and photons made it a good facility to search for and fully reconstruct both the signal mode,  $H^0 \rightarrow \Lambda p \pi^-$ , and the normalization mode,  $\Xi^0 \rightarrow \Lambda \pi_D^0$ , where  $\pi_D^0$  refers to the Dalitz decay of the  $\pi^0$  to  $e^+ e^- \gamma$ . For both modes, the  $\Lambda$ 's decay downstream of the parent particle's vertex to a  $p \pi^-$ . The data presented here were collected during two months of E799-II data taking in 1997.

The KTeV detector and the trigger configuration used to select events with four charged particles have been described elsewhere [10]. This Letter highlights aspects of the detector directly relevant to this analysis. A neutral beam, composed primarily of kaons and neutrons, was produced by focusing an 800 GeV/c proton beam at a vertical angle of 4.8 mrad on a 1.1 interaction length (30 cm) BeO target. Photons produced in the target were converted in a 7.6 cm lead absorber located downstream of the target. Charged particles were removed further downstream with magnetic sweeping. Collimators, followed by sweeping magnets, defined two 0.25  $\mu\text{sr}$  neutral beams that entered the KTeV apparatus (Fig. 1) 94 m downstream from the target. The 65 m vacuum ( $\sim 10^{-6}$  Torr) decay region extended to the first drift chamber.

The momenta of the charged particles were measured with a charged particle spectrometer, consisting of four planar drift chambers and a dipole analyzing magnet. The energies of the particles were measured with a high

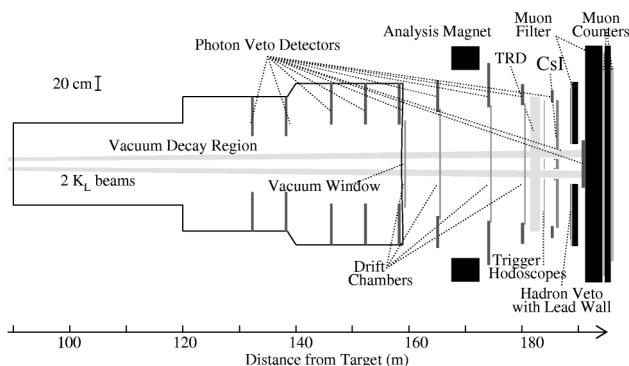


FIG. 1. Plan view of the KTeV spectrometer.

resolution CsI electromagnetic calorimeter. To distinguish electrons from hadrons, the energy ( $E$ ) measured by the calorimeter was compared to the momentum ( $p$ ) measured by the charged spectrometer. Electrons were identified by  $0.9 < E/p < 1.1$ , while pions and protons were identified by  $E/p < 0.9$ .

Off-line, events were required to have four reconstructed charged particles. We searched for long lived  $H^0$ 's which were produced at the target and decayed in the vacuum decay region. A characteristic feature of the topology of both the signal and normalization modes is that the parent particle's true decay vertex is defined by a charged track vertex, the  $p \pi^-$  vertex for the  $H^0$  and the  $e^+ e^-$  vertex for the  $\Xi^0$ . The subsequent  $\Lambda$ 's decay downstream of the parent particle's vertex to  $p \pi^-$ .

$H^0$  candidates were required to pass the following selection criteria. Downstream  $\Lambda$ 's were identified by requiring the ratio of the lab momenta of the  $p$  to  $\pi^-$  to be greater than 3, which accepted 99.8% of the simulated signal events. Because the  $\Lambda$  decays to two particles, the transverse momentum ( $P_T$ ) distribution of the decay products relative to the direction of the  $\Lambda$  exhibits a Jacobian peak at a maximum of 0.1 GeV/c. To enhance the selection of  $\Lambda$  decays relative to background three body  $K_L$  decays, where the  $P_T$  distribution is peaked at 0, we required the  $P_T$  of the  $p$  and the  $\pi^-$  to be between 0.07 and 0.11 GeV/c, accepting  $\sim 60\%$  of the simulated signal events. To select  $\Lambda$ 's further, we required the mass of the reconstructed  $p \pi^-$  to fall within  $\pm 5 \text{ MeV}/c^2$  of  $M_\Lambda$ , where the  $M_\Lambda$  resolution is  $\sim 1 \text{ MeV}/c^2$ . The charged portion of the upstream vertex is made up of a  $p$  and  $\pi^-$  and has kinematics similar to a  $\Lambda$  decay. Thus, the same constraint used for the  $\Lambda$  was applied, requiring the ratio of the lab momenta of the  $p$  to  $\pi^-$  to be greater than 3.

Interactions in the collimator, sweeping magnets, and vacuum window produced background events with multiple vertices. Events where at least one decaying particle was short lived were removed by requiring the reconstructed  $H^0$  and  $\Lambda$  vertices to be between 100 and 155 m from the target,  $\sim 5$  m away from those apparatus elements.

The signal region for  $H^0$  candidates was defined by requiring  $M_H$  to be between 2.190 and 2.235  $\text{GeV}/c^2$  to account for resolution effects in measuring  $M_H$ ; the upper and lower limits on  $M_H$  are 4  $\text{MeV}/c^2$  (more than twice our estimated  $M_H$  resolution) above the  $M_{\Lambda\Lambda}$  threshold of 2.231  $\text{GeV}/c^2$  and below the  $M_{\Lambda p \pi^-}$  threshold of 2.194  $\text{GeV}/c^2$ , respectively. In addition, the transverse momentum of the reconstructed  $H^0$  [ $P_T(H^0)$ ], measured relative to a vector connecting the  $H^0$  decay vertex and the target, was required to be less than 0.015 GeV/c (see Fig. 2). The cut on  $P_T(H^0)$  accepted 90% of the remaining simulated signal events. None of the events passed all the selection criteria.

To quantify the measurement sensitivity, we normalized to  $\Xi^0$  production, using data taken with the same

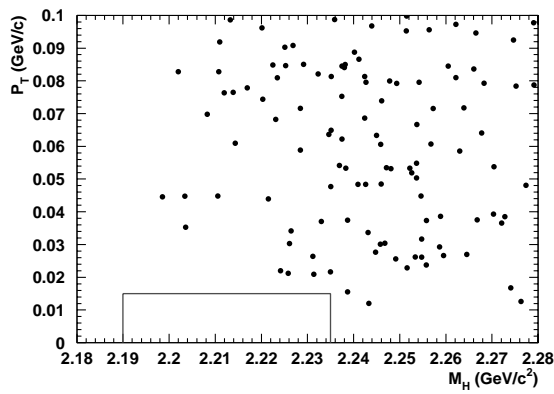


FIG. 2. The transverse momentum of the  $H^0$  versus  $M_H$  for events passing all the selection criteria except the cuts on  $P_T(H^0)$  and  $M_H$ . The box shows the signal region. The background events outside the signal region are from simultaneous decays of two particles in the fiducial volume, the predominant contribution coming from the decays  $K_L \rightarrow \pi^\pm l^\mp \nu$ .

trigger configuration as that for the  $H^0$  analysis, reconstructing  $\Xi^0 \rightarrow \Lambda \pi_D^0$  decays. Except for the additional photon coming from the  $\pi_D^0$ , the normalization mode's decay topology is similar to that of the  $H^0$ 's. Applying a series of cuts similar to those used for the  $H^0$  analysis yields 17 160  $\Xi^0$  events, with negligible background. The cleanliness of the normalization mode's signal is demonstrated in Fig. 3 which shows the  $\Xi^0$  invariant mass peak. Distributions of variables from simulated decays, such as the  $\Xi^0$ 's momentum and the location of the  $\Xi^0$ 's decay vertex, are consistent with the same for data.

The  $\Xi^0$  and  $H^0$  are expected to have different absorption lengths in the BeO target and the Pb absorber, leading to a difference in the transmission probability ( $T$ ) for the two particles. We estimate the  $\Xi^0$ -nucleon ( $\sigma_{\Xi N}$ ) and  $H^0$ -nucleon ( $\sigma_{HN}$ ) cross sections and thus the  $T$ 's based on the assumption of isospin invariance. In addition, we utilize measured  $np$ ,  $\Lambda p$ , and deuteron-proton ( $dp$ ) cross sections [11], 40, 35, and 75 mb, respectively, to account for the effect of replacing down quarks with strange quarks; we assume that the scale factor  $S = \sigma_{\Lambda p}/\sigma_{np}$  can be used to correct for the substitution of a single strange quark for a down quark and  $S^2$  for a double substitution. We then

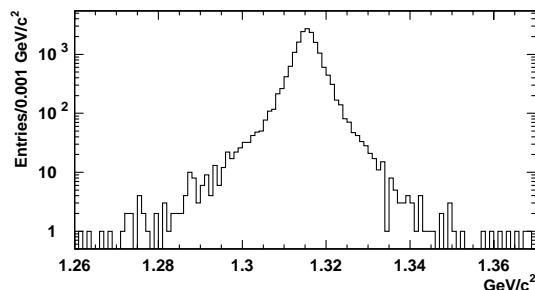


FIG. 3. The invariant mass of the  $\Lambda \pi_D^0$  sample used to normalize the signal mode ( $M_\Xi = 1.315$  GeV/ $c^2$ ). There are a total of 17 160 events in the mass peak.

estimate  $\sigma_{\Xi N}$  to be  $\sigma_{\Lambda p} S = (31 \pm 4)$  mb and  $\sigma_{HN}$  to be  $\sigma_{dp} S^2 = (57 \pm 18)$  mb, where the assigned errors are taken to be equal to the magnitude of the correction itself. The measured absorption lengths for nucleons in BeO and Pb are scaled by the factors  $\sigma_{np}/\sigma_{HN}$  and  $\sigma_{np}/\sigma_{\Xi N}$ . The estimated  $T$ 's in the target are  $T_{\Xi}^{\text{BeO}} = 0.623 \pm 0.037$  and  $T_H^{\text{BeO}} = 0.44 \pm 0.12$ . In the lead absorber, the  $T$ 's are estimated to be  $T_{\Xi}^{\text{Pb}} = 0.562 \pm 0.043$  and  $T_H^{\text{Pb}} = 0.35 \pm 0.14$ .

As no signal events passed all the selection criteria, the final result is presented as a 90% C.L. upper limit on the inclusive  $H^0$  production cross section over the solid angle defined by the collimators, expressed in terms of the inclusive  $\Xi^0$  production cross section

$$\frac{d\sigma_H}{d\Omega} < \frac{\xi}{N_{\Xi}} \frac{T_{\Xi}^{\text{BeO}}}{T_H^{\text{BeO}}} \frac{T_{\Xi}^{\text{Pb}}}{T_H^{\text{Pb}}} \frac{A_{\Xi}}{A_H} \frac{B(\Xi^0 \rightarrow \Lambda \pi_D^0)}{B(H^0 \rightarrow \Lambda p \pi^-)} \frac{d\sigma_{\Xi}}{d\Omega}, \quad (1)$$

where  $\xi$  is the factor which multiplies the single event sensitivity (SES) to give the 90% C.L. upper limit,  $N_{\Xi}$  is the number of reconstructed  $\Xi^0 \rightarrow \Lambda \pi_D^0$  decays, the various  $T$  factors are the transmission probabilities described previously,  $A_{\Xi}$  and  $A_H$  are the acceptances for  $\Xi^0$  and  $H^0$  decays, respectively, and  $B(\Xi^0 \rightarrow \Lambda \pi_D^0)$  and  $B(H^0 \rightarrow \Lambda p \pi^-)$  are the respective branching ratios. Our estimate of the SES suffers from a large relative uncertainty of  $\sim 50\%$ , predominantly due to the uncertainty in determining the transmission factors. The uncertainty in the SES gives rise to a factor of  $\xi = 3.06$  in the determination of the 90% C.L. upper limit [12].

The acceptances were determined from a detailed detector simulation. Because the trigger was the same for both the signal and the normalization modes and because both the signal and the normalization modes consist of four-track events with largely similar topologies, trigger and acceptance inefficiencies mostly cancel. The  $\Xi^0$  flux was measured using two separate triggers, each composed of different trigger elements. The discrepancy between the two flux measurements was converted into a systematic uncertainty in determining  $A_{\Xi}$ . Other systematic uncertainties were negligible relative to this uncertainty.  $A_{\Xi}$  was determined to be  $(6.93 \pm 0.94) \times 10^{-6}$ .

To determine  $A_H$ , the detector simulation included the  $H^0$  production spectrum proposed in Rotondo's phenomenological model [9]. The dominant experimental uncertainty in  $A_H$  comes from the simulation of proton showers in the calorimeter, where the relative uncertainty was determined to be 5.3%. For example, taking  $M_H$  in the middle of the mass range we are sensitive to,  $M_H = 2.21$  GeV/ $c^2$ , and the lifetime corresponding to the lifetime given in Ref. [5] for this mass,  $\tau_H = 5.28 \times 10^{-9}$  sec,  $A_H = 5.64 \times 10^{-3}$ . As a cross-check of Rotondo's model, which incorporates a  $\Xi^0$  production spectrum, we applied our measured  $\Xi^0$  production spectrum in the detector simulation, replacing

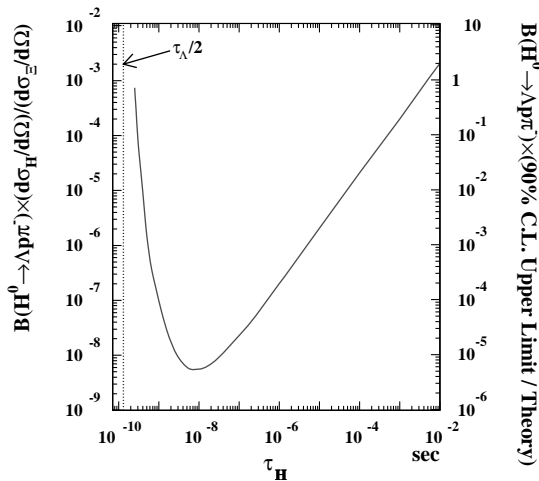


FIG. 4. The 90% C.L. upper limit on the ratio of the product of the  $H^0$  branching ratio and the production cross section to the  $\Xi^0$  production cross section as a function of the  $H^0$  lifetime.  $M_H$  is assumed to be 2.21 GeV/ $c^2$ . The sensitivity scale on the right ordinate axis assumes the production model of Ref. [9].

$M_{\Xi}$  and  $\tau_{\Xi}$  with  $M_H$  and  $\tau_H$ , respectively. This lowered  $A_H$  by  $\sim 15\%$ . The 90% C.L. upper limit on the product of the  $H^0$  branching ratio and the production cross section, taking into account all the uncertainties, is

$$B(H^0 \rightarrow \Lambda p \pi^-) \frac{d\sigma_H}{d\Omega} < 5.87 \times 10^{-9} \frac{d\sigma_{\Xi}}{d\Omega}. \quad (2)$$

In Fig. 4, we plot the 90% C.L. upper limit on the ratio  $[B(H^0 \rightarrow \Lambda p \pi^-) d\sigma_H/d\Omega]/(d\sigma_{\Xi}/d\Omega)$ , studying the effect on  $A_H$  of varying  $\tau_H$  over a large range of values. For short lifetimes, the  $H^0$ 's decay before reaching the decay region, while for long lived states, only a few decay while passing through the detector. Both effects lower our sensitivity to  $H^0$  decays. Varying  $M_H$  across the full range of masses to which we are sensitive leads to a relative shift of approximately  $\pm 60\%$  from the central value of the curve plotted in Fig. 4. Included in the figure is a line at  $\tau_{\Lambda}/2 = 1.316 \times 10^{-10}$  sec, the expected lifetime of a system made up of two lightly bound  $\Lambda$ 's, which might be a lower bound on  $\tau_H$ . To interpret the sensitivity of this result relative to the theoretical production model, we integrate the theoretical predictions for both  $d\sigma_H/d\Omega$  [9] and  $d\sigma_{\Xi}/d\Omega$  [13] over the solid angle covered by the collimators. The right ordinate axis of Fig. 4 shows the sensitivity of this measurement. Thus, assuming Rotondo's production model, our result rules out lightly bound  $H^0$ 's, between the  $M_{\Lambda p \pi^-}$  and  $M_{\Lambda\Lambda}$  thresholds of 2.194 and 2.231 GeV/ $c^2$ , respectively, over a large range of lifetimes, from  $\sim 5 \times 10^{-10}$  sec up to  $\sim 1 \times 10^{-3}$  sec.

A model proposed in Ref. [5] associates  $M_H$  with both  $\tau_H$  and  $B(H^0 \rightarrow \Lambda p \pi^-)$ . For example, for  $M_H = 2.21$  GeV/ $c^2$  they predict  $\tau_H = 5.28 \times 10^{-9}$  sec and a branching ratio of  $5.4 \times 10^{-2}$ . To test this model, we vary  $M_H$  between the  $M_{\Lambda p \pi^-}$  and  $M_{\Lambda\Lambda}$  thresholds,

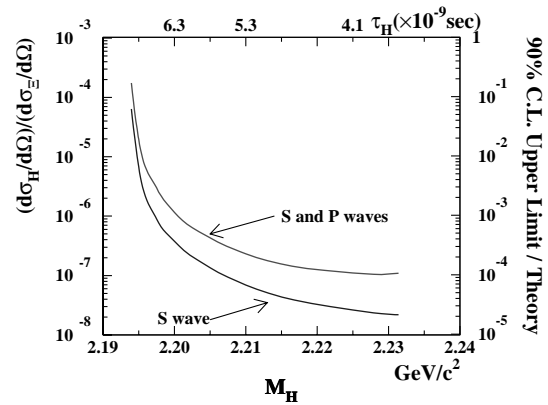


FIG. 5. The 90% C.L. upper limit on the ratio of the  $H^0$  production cross section to the  $\Xi^0$  production cross section as a function of  $M_H$ . The top abscissa axis shows the  $H^0$  lifetime associated with  $M_H$  assuming the  $H^0$ 's wave function is a pure  $S$  wave state, as predicted in Ref. [5]. If the  $H^0$  contains both  $S$  and  $P$  wave contributions, Ref. [5] estimates the lifetime could be as low as half the lifetime of the pure  $S$  wave state, worsening our sensitivity to the  $H^0$ . The curve for the  $S$  and  $P$  wave state is derived using half the lifetime of the pure  $S$  wave.

determining the dependence of the production cross section on the mass, lifetime, and branching ratio. Figure 5 is a plot of  $(d\sigma_H/d\Omega)/(d\sigma_{\Xi}/d\Omega)$  versus  $M_H$ . In this figure, the factor influencing the sensitivity the most is the  $H^0$  branching ratio which decreases from a maximum of 14% at the  $M_{\Lambda\Lambda}$  threshold down to zero at the  $M_{\Lambda p \pi^-}$  threshold. The right ordinate axis of Fig. 5 shows the sensitivity of this measurement, based on Rotondo's model. Assuming Rotondo's production model, this result excludes a long lived  $H^0$  state, as proposed in Ref. [5], for  $M_H$  between the  $M_{\Lambda p \pi^-}$  and  $M_{\Lambda\Lambda}$  thresholds.

To conclude, in the context of published models, our result excludes a lightly bound  $H^0$  dibaryon over a range of mass below the  $M_{\Lambda\Lambda}$  threshold not ruled out by previous experiments and for a wide range of lifetimes, placing stringent limits on the  $H^0$  production process. At the 90% C.L. upper limit, this result, in conjunction with the result from experiment BNL E888 [8], rules out the model proposed in Ref. [5] for all  $\Delta S = 1$  transitions.

We thank D. Ashery, F. S. Rotondo, and A. Schwartz for their insightful comments. We gratefully acknowledge the support and effort of the Fermilab staff and the technical staffs of the participating institutions for their vital contributions. This work was supported in part by the U.S. Department of Energy, The National Science Foundation, and The Ministry of Education and Science of Japan.

\*To whom correspondence should be addressed.

Electronic address: bendavid@htc.com.

†Present address: The Hull Group, L.L.C., Chicago, IL 60606.

‡On leave from C.P.P. Marseille/C.N.R.S., France.

[1] R. L. Jaffe, Phys. Rev. Lett. **38**, 195 (1977).

- [2] H. J. Lipkin, Phys. Lett. B **195**, 484 (1987); C. Gignoux *et al.*, Phys. Lett. B **193**, 323 (1987); J. Leandri *et al.*, Phys. Rev. D **51**, 3628 (1995).
- [3] H. J. Lipkin, Phys. Lett. B **198**, 131 (1987).
- [4] B. Quinn *et al.*, in *Proceedings of Baryons'92: International Conference on the Structure of Baryons and Related Mesons, New Haven, Connecticut, 1992*, edited by M. Gai (World Scientific, River Edge, NJ, 1993), p. 278. For a comprehensive listing of current theoretical predictions see R. W. Stotzer, Ph.D. dissertation, University of New Mexico, 1997 (unpublished).
- [5] J. F. Donoghue, E. Golowich, and B. R. Holstein, Phys. Rev. D **34**, 3434 (1986).
- [6] D. Ashery, in *Proceedings of Hadron Spectroscopy: Seventh International Conference, Upton, New York, 1997*, edited by S. U. Chung and H. J. Willutzki (American Institute of Physics, Woodbury, NY, 1998), p. 293.
- [7] J. K. Ahn *et al.*, Phys. Lett. B **378**, 53 (1996); R. W. Stotzer *et al.*, Phys. Rev. Lett. **78**, 3646 (1997).
- [8] J. Belz *et al.*, Phys. Rev. Lett. **76**, 3277 (1996). Addendum in J. Belz *et al.*, Phys. Rev. C **56**, 1164 (1997).
- [9] F. S. Rotondo, Phys. Rev. D **47**, 3871 (1993).
- [10] J. Adams *et al.*, Phys. Rev. Lett. **80**, 4123 (1998).
- [11] Particle Data Group, C. Caso *et al.*, Eur. Phys. J. C **3**, 1 (1998).
- [12] R. D. Cousins and V. L. Highland, Nucl. Instrum. Methods Phys. Res., Sect. A **320**, 331 (1992).
- [13] L. G. Pondrom, Phys. Rep. **122**, 57 (1985).